Single-cell determination of iron content in magnetotactic bacteria: implications for the iron biogeochemical cycle

Matthieu Amor^{a*}, Mickaël Tharaud^b, Alexandre Gélabert^b, Arash Komeili^{a,c*}

^a Department of Plant and Microbial Biology, University of California, Berkeley, CA 94720-3102

^b Institut de Physique du Globe de Paris, Sorbonne Paris Cité, Univ. Paris Diderot, UMR 7154 CNRS, 1 rue Jussieu, 75238 Paris, France

^c Department of Molecular and Cell Biology, University of California, Berkeley, CA 94720-3200

*Corresponding authors: amor@ipgp.fr (MA); komeili@berkeley.edu (AK)

Classification: Physical Sciences

Category: Earth, Atmospheric and Planetary Sciences

Keywords: Magnetotactic bacteria, Biomineralization, Single-Cell – Inductively Coupled Plasma – Mass Spectrometry, Iron biogeochemical cycle

Abstract

Magnetotactic bacteria (MTB) are ubiquitous aquatic microorganisms that biomineralize dissolved iron from the environment into intracellular nanoparticles of magnetite $[Fe(II)Fe(III),O_4]$ or greigite $[Fe(II)Fe(III),S_4]$ in a genetically controlled manner. After cell death, these magnetite and greigite crystals are trapped into sediments which effectively removes iron from the soluble pool. MTB may significantly impact the iron biogeochemical cycle, especially in the ocean where dissolved iron limits nitrogen fixation and primary productivity. Although MTB are ubiquitous in the environment, their impact on the biogeochemical cycling of metallic elements is still poorly constrained. A thorough assessment of the mass of iron incorporated by MTB has been hampered by a lack of methodology to accurately measure the amount of, and variability in, their intracellular iron content. Here, we quantify the mass of iron contained in single MTB cells of the model organism, Magnetospirillum magneticum sp. AMB-1, using a time-resolved mass spectrometry methodology. Bacterial iron content depends on the external iron concentration, and reaches a maximum value of 10⁻⁶ ng of iron per cell when bacteria are cultivated with initial iron concentrations of 100 µM or higher. From our experimental results, we calculated the flux of dissolved iron incorporation into natural MTB populations and conclude that MTB may mineralize a significant fraction of environmental dissolved iron into crystals.

Significance statement

Magnetotactic bacteria (MTB) are the only known bacterial species that form intracellular iron crystals in a genetically controlled manner and are observed in all aquatic environments. When the bacteria die, their crystals can be trapped into sediments and the iron they contain is, at least temporally, lost from the environment. MTB could thus prevent other organisms from accessing iron, which is an essential nutrient. To determine whether MTB significantly impact iron in the environment, we developed a mass spectrometry methodology to quantify the iron content in individual bacterial cells cultivated in the laboratory. We then show that MTB populations in the environment may incorporate a mass of iron that is of the same order of magnitude as the amount of bioavailable iron delivered to the ocean.

\body

Iron is one of Earth's most abundant element and an essential constituent for all living organisms. Before the Great Oxidation Event ~2.5 Ga ago, the atmosphere and hydrosphere redox state was such that iron could accumulate in the hydrosphere as soluble reduced Fe(II) species, thus available to living organisms for metabolic purposes (1). Later, oxygen accumulation at the Earth surface led to Fe(II) oxidation into insoluble Fe(III) and a dramatic decrease in the concentration of bioavailable iron (2). Biological organisms adapted to these changing environmental conditions by developing new strategies for accessing iron to sustain their metabolic activity, e.g. secreting soluble organic compounds binding iron. Indeed, although nitrogen and phosphorus are usually considered to be the nutrients limiting biomass production, iron has been demonstrated to limit nitrogen fixation and primary production in large open "High Nutrient, Low Chlorophyll" ocean surfaces (3, 4). Iron fertilization in these regions, as well as in laboratory experiments, leads to higher primary production and chlorophyll content (e.g. 3-5). Dissolved iron concentration in the ocean thus controls carbon and nitrogen fixation into the biomass.

Magnetotactic bacteria (MTB) are ubiquitous microorganisms observed in all modern aquatic environments. MTB, which can represent up to 30% of the total microbial biomass in some microhabitats (6), take up dissolved iron from their environment and precipitate it as intracellular nanoparticles of magnetite [Fe(II)Fe(III)₂O₄] or greigite [Fe(II)Fe(III)₂S₄] via a genetically controlled pathway (7). Magnetite or greigite crystals are arranged as chains inside the cell, and provide the bacteria with a magnetic dipole for

navigation purposes (7). In sediments or water column, MTB are markers of oxic/anoxic transition zones (OATZ) where the concentration of dissolved iron is at its maximum (8, 9). MTB have been proposed to represent some of the most ancient organisms capable of biomineralization, with an origin dating back to at least 3 Ga (10). Although MTB are ubiquitous on Earth, their impact on the past and modern biogeochemical cycling of metallic elements is still poorly constrained. The significance of MTB rises from their capacity to sequester dissolved iron in crystals. When the cells die, the magnetite and greigite crystals are trapped into sediments (11). Therefore, MTB potentially lower the concentration of dissolved iron in aquatic environments such as oceans and prevent other organisms from accessing an available pool of iron.

Previous works proposed to quantify the total mass of iron contained in natural MTB populations to assess their impact on the iron biogeochemical cycle (6, 12) but some parameters required for such estimations are still unknown. The critical step for quantifying the role of MTB on the iron biogeochemical cycle is to determine their iron content. To date, no analytical methodology can achieve the measurement of bacterial iron mass at the cellular level. The mass of iron in a single magnetotactic cell has mainly been estimated from measurement of the volume of magnetite observed with electron microscopy (*e.g.* 6, 13). Iron isotope studies of MTB suggested that a large fraction (~50%) of the total cellular iron could be located in a reservoir distinct from magnetite (14, 15), such that the mass of magnetite in MTB cells is not an accurate estimate of the total mass of iron they contain. Estimation of total iron in MTB cells from measurement of total bacterial iron in a given population is also prone to biases. Such methodology can only estimate the mean iron content, and cannot determine variability in a given MTB

population. Recently, time-resolved Inductively Coupled Plasma – Mass Spectrometry has drawn interest for single-cell characterization of biological samples. Instead of a measurement of bulk cellular iron dissolved in acid solutions, this technique allows for the introduction of whole intact cells to the plasma for the detection of their corresponding ionized iron clouds, each corresponding to the content of an individual cell. Such mass spectrometry technique enables the analysis of a large number of cells corresponding to a given population (e.g. 10⁴ cells per milliliter of solution in the present study), thus providing strong statistical insights. It has been used for analyses of large eukaryotic cells, but only a handful of bacterial characterizations were carried out in which iron could not be detected (16). In the present study, we performed Single-Cell – Inductively Coupled Plasma - Mass Spectrometry (SC-ICP-MS) measurements to determine the mass of iron contained in cells of the magnetotactic bacterium Magnetospirillum magneticum strain AMB-1 cultivated at different initial iron concentrations. Bacterial iron content ranged between ~0.5 and 1 10⁻⁹ ng/cell. The length of magnetite crystals produced by AMB-1 strongly correlated with both external iron concentration and bacterial iron content. Using these experimental findings, we estimate that environmental MTB populations incorporate a significant amount of iron which may be equivalent in magnitude to iron inputs into oceans.

Results and Discussion

Iron content in single AMB-1 cells

AMB-1 was cultivated at initial iron concentrations ranging between 10 and 500

5

µM for two or four days (see supplementary materials). After cultures, cells were recovered and washed three times using a phosphate buffer (PBS) to remove iron potentially adsorbed on the cell surfaces. We ensured that no iron leaked outside of the cells before analyses, and the iron mass balance of the experiments was checked to demonstrate that all iron fractions were recovered. Bacteria were then analyzed for their iron content. All experiments were carried out in triplicates. The distributions of iron content in the different AMB-1 populations showed contrasting patterns depending on the initial iron concentration conditions (Fig. 1). Data were consistent after 2 and 4 days of culture for a given initial iron concentration in the external solution. At 10 µM of iron in the external medium, bacterial iron content showed low variability between the different cells (Fig. 1). The mass of iron per cell ranged from $\sim 0.07 \times 10^{-6}$ to 0.7×10^{-6} ng/cell (table S1). The variability between cells increased at higher initial iron concentration in the growth medium, with cellular iron content ranging from $\sim 0.2 \times 10^{-6}$ to 2×10^{-6} ng/cell at 50 μM , and $\sim 0.1 \times 10^{-6}$ to 2 \times 10⁻⁶ ng/cell at 100 μM . For higher initial iron concentrations in the external medium, distribution and variability patterns of bacterial iron contents were similar to the 100 uM condition. From the distributions shown in figure 1, we calculated a mean bacterial iron content in AMB-1 populations corresponding to each experimental condition. The mass of iron incorporated into AMB-1 cells showed a logarithmic increase with increasing external iron concentration (Figs. 1, 2 and table S1). Mean values ranged between $\sim 0.35 \times 10^{-6}$ and 1.20×10^{-6} ng/cell when bacteria were cultivated for two days. Cellular iron content was similar after four days of culture, although consistent lower values were observed (Fig. S1 and table S1). This observation indicates that some bacterial iron could be lost during growth in culture, a finding in good agreement with previous studies that proposed Fe(II) diffusion between the bacterial internal medium and the external solution (15). The maximum bacterial iron content was reached at 100 μ M of iron in the initial external medium, with a mass of iron per cell of $\sim 1 \times 10^{-6}$ ng/cell, and no increase in intracellular iron was observed for higher initial iron concentrations (Fig. 2).

We next wanted to determine whether iron uptake is strictly linked to magnetite biomineralization, or if a potential additional iron pool, distinct from magnetite, exists in AMB-1. Magnetosome formation and magnetite precipitation in AMB-1 require ~30 genes that are necessary and sufficient for biomineralization, and are contained in a specific portion of the genome called the magnetosome gene island (MAI) (7). We used a mutant AMB-1 strain lacking MAI (ΔMAI strain), which is unable to form magnetosomes and shows no magnetic-sensitive behavior (17) (see supplementary materials). This mutant AMB-1 strain was cultivated in the same experimental conditions as the wild-type strain, and analyzed for its iron content. Iron content distributions in ΔMAI bacteria were similar in all experimental conditions, although the number of cells detected by the spectrometer was lower compared to non-mutant AMB-1 (Fig. S4, table S3). This could be explained by two hypotheses: (i) the iron content in some of the Δ MAI cells was below the detection limit (i.e. 1.75×10^{-8} ng/cell, see supplementary materials), or (ii) a more efficient growth for non-mutant cells compared to the ΔMAI AMB-1. Growth curves for the two strains indicated a consistent higher optical density (400 nm) for the non-mutant bacteria, illustrating a higher bacterial density (table S4). This shows that experimental results can be at least partially explained by the less efficient growth for the Δ MAI strain. It is important to note, however, that the difference in optical density does not account for the difference in cell number as measured by the mass spectrometer. Thus, we predict that the Δ MAI cultures, as compared to wild-type cell cultures, contained more cells with iron contents below the detection of the mass spectrometer. Nevertheless, the mean mass of iron in Δ MAI cells ranged between 1.73×10^{-7} and 5.08×10^{-7} ng/cell (table S3), corresponding to 20-40% of the mass of iron contained in non-mutant cells (Fig. S4). This shows that AMB-1 cells unable of forming magnetosomes can still incorporate a significant mass of iron.

Magnetite length as a proxy for external iron concentration and bacterial iron content

Magnetite length strongly correlated with both external iron concentration and the mass of iron in bacteria (Fig. 3). The mean size of magnetite nanoparticles measured with transmission electron microscopy (see supplementary materials) increased from 28.5 ± 0.5 nm in AMB-1 cells cultivated at an initial iron concentration of $10 \mu M$ to 35 ± 0.7 nm when bacteria were cultivated at $500 \mu M$ (table S2), corresponding to an average intracellular iron content of $\sim 0.35 \times 10^{-6}$ and 1.20×10^{-6} ng/cell, respectively. The magnetite length was logarithmically correlated with the external initial iron concentration, whereas it showed an exponential-like increase with increasing bacterial iron content (Fig. 3). The general picture of iron cycling in AMB-1 suggests that iron is first transported to the additional iron pool, distinct from magnetite, before its precipitation in magnetosomes (15). Our results are in good agreement with this model, as they indicate a delay in magnetite precipitation as iron incorporation in AMB-1 increases. Overall, they show that magnetite length could be useful for paleo-

environmental reconstructions (9), in which fossils of MTB corresponding to their mineralogical remains could be used to determine the concentration of iron in ancient fluids hosting MTB as well as the mass of iron in MTB cells.

Implication for natural MTB populations and the iron biogeochemical cycle

Based on our experimental results, we can propose an estimate for the global mass of iron contained in environmental MTB populations (M_{MTB}) by utilizing the MTB concentration in various aqueous environments, the global volume of water hosting MTB (V_{MTB}) and the mass of iron in MTB cells (M_{Fe}):

$$M_{MTB} = M_{Fe} C_{MTB} V_{MTB} \tag{1}$$

The concentration of MTB is different between freshwater ($10^5 \le C_{MTB} \le 10^7$ cells/cm³), seawater ($10^3 \le C_{MTB} \le 10^5$ cells/cm³), and estuaries ($10^4 \le C_{MTB} \le 10^7$ cells/cm³) (*e.g.* 13, 18-22). The volume of water containing MTB (V_{MTB}) can be expressed as the sum of the surfaces of freshwater (4.16×10^{16} cm²), seawater (3.63×10^{18} cm²) or estuaries (1.1×10^{16} cm²) (23-25), multiplied by the thickness of OATZ. For a 1-cm thick OATZ, V_{MTB} corresponding to the freshwater, seawater and estuaries is of 4.6×10^{16} , 3.6×10^{18} and 1×10^{16} cm³, respectively. In order to calculate the most conservative estimates of M_{MTB} , we considered the lowest mass of iron per cell we measured in AMB-1 (*i.e.* ~ 0.5×10^{-6} ng/cell, corresponding to an initial iron concentration of $10 \mu M$). Analyses of AMB-1 cells cultivated with no iron added to the growth medium showed similar values to the $10 \mu M$ condition (see supplementary materials, table S5), showing that 0.5×10^{-6} ng/cell is

an appropriate conservative estimate of bacterial iron content. The dissolved iron concentration in the ocean is also low, but MTB observed in marine environments show chains of magnetite containing 10-20 crystals as in AMB-1 (26). M_{MTB} can thus be estimated for MTB populations in freshwater $(2.5 \times 10^3 \le M_{MTB} \le 2.5 \times 10^5 \text{ kg})$, oceans (2 \times 10³ \leq M_{MTB} \leq 2 \times 10⁵ kg), and estuaries (6 \times 10¹ \leq M_{MTB} \leq 3 \times 10⁴ kg). To convert this mass estimate into a flux, we use a turnover time of MTB populations of 2 days measured in environmental bacteria (i.e. corresponding to the time needed for doubling the total mass of iron incorporated by MTB populations) (12), leading to a flux of iron processed by MTB of $4 \times 10^5 \le M_{MTB} \le 4 \times 10^7$ kg per year for freshwater, $3.3 \times 10^5 \le M_{MTB} \le 3.3 \times 10^5$ 10^7 kg per year for the ocean, and $10^4 \le M_{\rm MTB} \le 5 \times 10^6$ kg per year for estuaries. Shorter turnover times were proposed for natural MTB populations (i.e. one division every twelve hours for each cell), but they may correspond to an exponential phase of growth that is probably not representative of natural environments (27). The most variable parameter in our calculations corresponds to the OATZ thickness. In various environmental settings, MTB populations were observed to span over a few-meter thick OATZ (11, 13, 22, 28). Therefore, our estimate of the flux of iron processed each year by MTB is most likely conservative. Using thicker estimates for the OATZ in estuaries in which MTB thrive (i.e. up to a few meters) (11, 13, 22), the flux of dissolved iron incorporated by MTB increases up to $5 \times 10^5 \le M_{MTB} \le 2.5 \times 10^8$ kg per year (50-cm thick OATZ) and $10^6 \le M_{\rm MTB} \le 5 \times 10^8$ kg per year (1-m thick OATZ) kg/yr. We also note that AMB-1 produces less nanoparticles (~15 per cell) than MTB observed in natural environmental settings which can produce up to five hundred nanocrystals per cells, including greigite-forming MTB (13). This reinforces the conservative character of our estimate, and shows that AMB-1 is appropriate to model natural samples. Lin and collaborators proposed a conservative estimate of iron uptake by lacustrine and world MTB of 2×10^6 and 1×10^8 kg per year, respectively, which falls within our estimates (6).

Finally, to assess the impact of MTB populations on the iron biogeochemical cycle, we compared our results with the main three inputs of dissolved iron to the oceans (Fig. 4): rivers ($\sim 1.5 \times 10^8$ kg/yr), hydrothermalism ($\sim 3 \times 10^8$ kg/yr), and atmospheric dust ($\sim 5 \times 10^8$ kg/yr) (29). Given that we consider only the most conservative estimations, this shows that MTB can incorporate a significant fraction of the mass of dissolved iron transported to the ocean. In estuarine environments, the estimated mass of dissolved iron incorporated by bacteria corresponds to 1-500 % of the mass of dissolved iron transported by the rivers. MTB could thus act as a sink of iron in these environments and prevent accumulation of riverine dissolved iron in the ocean (11). We note that dissolved iron corresponds to a small fraction of the total iron transported by rivers (less than 1%; see ref. 29). Iron mineral phases could thus dilute MTB nanoparticles in sediments, although magnetite and greigite crystals likely produced by MTB have been magnetically identified in estuarine samples (11, 30).

In sum, chemical and microbial data show that MTB may play an important role by transferring a significant fraction of dissolved, bioavailable iron to stable solid phases in sediments (Fig. 4). This precipitation flux could limit primary production in oceanic regions. Given that a significant fraction of iron is not precipitated as magnetite or greigite in MTB, it remains to be determined whether some of the iron assimilated by bacteria can be released to the environment after the cell death. This fraction could

correspond to iron associated with organic compounds that include proteins. Iron isotope

work on MTB showed a specific enrichment in heavy isotopes of the iron fraction

associated with these proteins (14, 15), in good agreement with iron isotope data obtained

from environments in which MTB populations were observed (31, 32). This suggests that

MTB could control partly the dissolved iron isotope budget in the environment, and that

iron isotopes could be used as a tool for probing iron released and/or precipitated by

MTB. In the future, direct measurements of the division times of environmental MTB

populations and a more accurate picture of the biogeography of their distribution will

yield a more accurate estimate of the impact of MTB on environmental fate and cycling

of iron.

Material and methods

Detailed procedures for AMB-1 culture, electron microscopy characterizations and

chemical analyses are provided in the supplementary materials.

ACKNOWLEDGMENTS. AK and MA are supported by grants through the National

Science Foundation (1504681) and National Institutes of Health (R01GM084122 and

R35GM127114). Part of this work was supported by IPGP multidisciplinary program

12

PARI and by Region Île-de-France SESAME Grant no. 12015908.

References

- 1. Lyons TW, Reinhard CT, Planavsky NJ (2014) The rise of oxygen in Earth's early ocean and atmosphere *Nature* 506: 307-315.
- 2. Knoll AH, Nowak MA (2017) The timetable of evolution. *Sci. Adv.* 3: e1603076.
- 3. Coale KH *et al* (2004) Southern Ocean iron enrichment experiment: carbon cycling in high- and low-Si waters. *Science* 304 408-414.
- 4. Martínez-García A, Sigman DM, Ren H, Anderson RF, Straub MS, Hodell DA, Jaccard SL, Eglinton TI, Haug GH (2014) Iron fertilization of the subantartic ocean during the last ice age. *Science* 343: 1347-1350
- 5. Jacq V, Ridame C, L'Helguen S, Kaczmar F, Saliot A (2014) Response of the unicellular diazotrophic cyanobacterium *Crocosphaera watsonii* to iron limitation. *PLoS One* 9: 10.1371/journal.pone.0086749.
- 6. Lin W, Bazylinski DA, Xiao T, Wu L-F, Pan Y (2014) Life with compass: diversity and biogeography of magnetotactic bacteria. *Environ. Microbiol.* 16: 2646-2658.
- 7. Uebe R, Schüler D (2016) Magnetosome biogenesis in magnetotactic bacteria. *Nat. Rev. Microbiol.* 14: 621-637.
- 8. Lefèvre CT, Bazylinski DA (2013) Ecology, diversity, and evolution of magnetotactic bacteria. *Microbiol Mol. Biol. Rev.* 77: 497-526.
- 9. Kopp RE, Kirschvink JL (2008) The identification and biogeochemical interpretation of fossil magnetotactic bacteria. *Earth Sci. Rev.* 86: 42-61.
- 10. Lin W, Paterson GA, Zhu Q, Wang Y, Kopylova E, Li Y, Knight R, Bazylinski DA, Zhu R, Kirschvink JL, Pan Y (2017) *Proc. Natl. Acad. Sci. U.S.A.* 114: 2171-2176.
- 11. Chen AP, Berounsky VM, Chan MK, Blackford MG, Cady C, Moskowitz BM, Kraal P, Lima EA, Kopp RE, Lumpkin GR, Weiss BP, Hesse P, Vella NGF (2014) Magnetic properties of uncultivated magnetotactic bacteria and their contribution to a stratified estuary cycle. *Nat. Commun.* 5: 10.138/ncomms5797.
- 12. Simmons SL, Edwards KJ (2006) Geobiology of magnetotactic bacteria. *Microbiol. Monogr.* 3: 10.1007/7171_039.
- 13. Simmons SL, Bazylinski DA, Edwards KJ (2007) Population dynamics of marine magnetotactic bacteria in a meromictic salt pond described with qPCR. *Environm*. *Microbiol*. 9: 2162-2174.
- 14. Amor M, Busigny V, Louvat P, Gélabert A, Cartigny P, Durand-Dubief M, Ona-Nguema G, Alphandéry E, CHebbi I, Guyot F (2016) Mass-dependent and independent signature of Fe isotopes in magnetotactic bacteria. *Science* 352: 705-708.
- 15. Amor M, Louvat P, Tharaud M, Gélabert A, Cartigny P, Carlut J, Isambert A, Durand-Dubief M, Ona-Nguema G, Alphandéry E, Chebbi I, Guyot F (2018) Iron uptake and magnetite biomineralization in the magnetotactic bacterium *Magnetospirillum magneticum* strain AMB-1: an iron isotope study. *Geochem. Cosmochem. Acta* 232: 225-243.
- 16. Miyashita S-i, Groombridge AS, Fujii S-i, Minoda A, Takatsu A, Hioki A, Chiba K, Inagaki K (2014) Highly efficient single-cell analysis of microbial cells by

- time-resolved inductively coupled plasma mass spectrometry. J. Anal. At. Spectrom. 29: 1598-1606.
- 17. Murat D, Quinlan A, Vali H, Komeili A (2010) Comprehensive genetic dissection of the magnetosome gene island reveals the step-wise assembly of a prokaryotic organelle. *Proc. Natl. Acad. U.S.A.* 107: 5593-5598.
- 18. Spring S, Amann R, Ludwig W, Schleifer KH, van Gemerden H, Petersen N (1993) Dominating role of an unusual magnetotactic bacterium in the microaerobic zone of a freshwater sediment. *Appl. Environ. Microbiol.* 59: 2397-2403.
- 19. Flies CB, Jonkers HM, de Beer D, Bosselmann K, Böttcher ME, Schüler D (2005) Diversity and vertical distribution of magnetotactic bacteria along chemical gradients in freshwater microcosms. *FEMS Microbiol. Ecol.* 52: 185-195.
- 20. Blakemore RP (1982) Magnetotactic bacteria. Ann. Rev. Microbiol. 36: 217-238.
- 21. Bazylinski DA, Frankel RB, Heywood BR, Mann S, King JW, Donaghay PL, Hanson AK (1995) Controlled biomineralization of magnetite (Fe₃O₄) and greigite (Fe₃S₄) in a magnetotactic bacterium. *Appl. Environ. Microbiol.* 61: 3232-3239.
- 22. Simmons SL, Sievert SM, Frankel RB, Bazylinski DA, Edwards KJ (2004) Spatiotemporal distribution of marine magnetotactic bacteria in a seasonally stratified coastal salt pond. *Appl. Environ. Microbiol.* 70: 6230-6239.
- 23. Downing JA, Prairie YT, Cole JJ, Duarte CM, Tranvik LJ, Striegl RG, McDowell WH, Kortelainen P, Caraco NF, Melack JM, Middelburg JJ (2006) The global abundance and size distribution of lakes, ponds, and impoundments. *Limnol. Oceanogr.* 51: 2388-2397.
- 24. Regnier P *et al* (2013) Anthropogenic perturbation of the carbon fluxes from land to ocean. *Nat. Geosci.* 6: 10.1038/NGEO1830.
- 25. Cogley JG (2012) Area of the ocean. *Mar. Geod.* 35: 379-388.
- 26. Liu J *et al* (2017) Bacterial community structure and novel species of magnetotactic bacteria in sediments from a seamount in the Mariana volcanic arc. *Sci. Rep.* 7: 10.1038/s41598-017-17445-4.
- 27. Moench TT, Konetzka WA (1978) A novel method for the isolation and study of a magnetotactic bacterium. *Arch. Microbiol.* 119: 203-212.
- 28. Rivas-Lamelo S, Benzerara K, Lefèvre CT, Monteil CL, Jézéquel D, Menguy N, Viollier E, Guyot F, Férard C, Poinsot M, Skouri-Panet F, Trcera N, Miot J, Duprat E (2017) Magnetotactic bacteria as a new model for P sequestration in the ferruginous Lake Pavin. *Geochem. Persp. Let.* 5: 35-41.
- 29. Fantle MS, DePaolo DJ (2004) Iron isotopic fractionation during continental weathering. *Earth Planet*. *Sci. Lett.* 228: 547-562.
- 30. Ouyang T, Li M, Appel E, Fu S, Jia G, Li W, Zhu Z (2017) Magnetic properties of surface sediments from the Pearl River Estuary and its adjacent waters: implication for provenance. *Mar. Geol.* 390: 80-88.
- 31. Chen J-B, Busigny V, Gaillardet J, Louvat P, Wang Y-N (2014) Iron isotopes in the Seine River (France): natural versus anthropogenic sources. *Geochem. Cosmochem. Acta* 128: 128-143.
- 32. Ilina SM, Poitrasson F, Lapitskiy SA, Alekhin YV, Viers J, Pokrovsky OS (2013) Extreme iron isotope fractionation between colloids and particles of boreal and temperate organic-rich waters. *Geochem. Cosmochem. Acta* 101: 96-111.

Figure captions

Fig. 1. Mass of iron per cell measured in AMB-1 populations cultivated at (A) 10, (B) 50,

(C) 100, (D) 200, (E) 300 or (F) 500 µM of Fe(III).

Fig. 2. Mass of iron per AMB-1 cell cultivated for two days versus initial Fe(III)

concentration in the external medium. Each symbol represents the mean value of three

replicates ± 1SD. The mass of iron per cell shows a logarithmic increase with higher iron

concentration in AMB-1 growth medium (correlation coefficient of 0.92).

Fig. 3. Magnetite length in AMB-1 versus (A) Initial Fe(III) concentration in the external

medium and (B) mass of iron per cell. Each point corresponds to the mean value of two

replicates ± 1SD. At least 300 magnetite nanoparticles corresponding to a given

population were measured. Magnetite length shows logarithmic and exponential increase

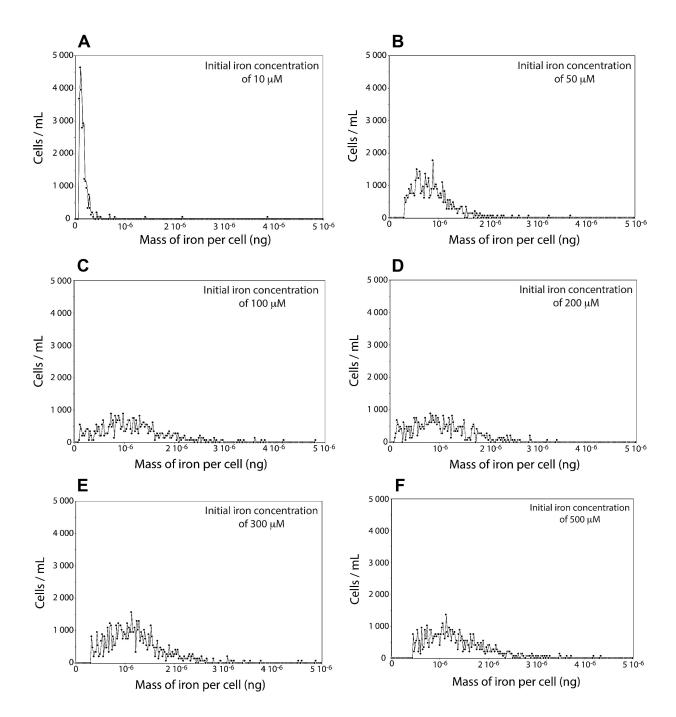
with Fe(III) concentration in the external medium (correlation coefficient of 0.97) and

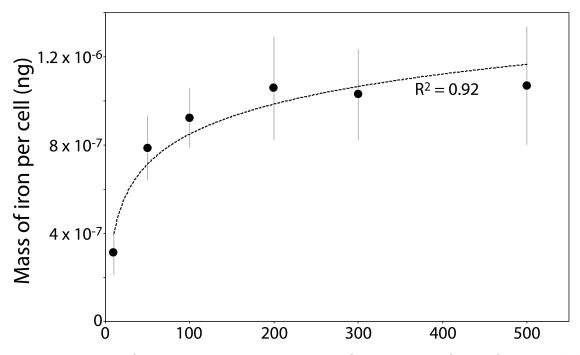
mass of iron per cell (correlation coefficient of 0.98), respectively.

Fig. 4. Model indicating the main inputs of dissolved iron to the oceans (in red, data from

ref. 29) and the fluxes of iron incorporation by magnetotactic bacteria (in blue, data from

this study). All flux numbers are given in kg of iron pear year.





Initial iron concentration in the external medium (μM)

